Osteoarthritis and Cartilage 31 (2023) 374–385

Osteoarthritis and Cartilage

Ribosomal RNA-based epitranscriptomic regulation of chondrocyte translation and proteome in osteoarthritis

A. Chabronova †, G.G.H. van den Akker †, B.A.C. Housmans †, M.M.J. Caron †, A. Cremers †, D.A.M. Surtel †, K. Wichapong ‡, M.M.J. Peffers §, L.W. van Rhijn †, V. Marchand ‖, Y. Motorin ‖ ¶, T.J.M. Welting † *

† *Laboratory for Experimental Orthopedics, Department of Orthopedic Surgery, Maastricht University, Maastricht, the Netherlands*
‡ *Cardiovascular Research Institute Maastricht (CARIM), Department of Biochemistry, Maastricht University, Maastricht, the Netherlands*
§ *Institute of Life Course and Medical Sciences, University of Liverpool, Liverpool, UK*
‖ *Université de Lorraine, UAR2008 IBSLor CNRS-INSERM, BioPole, Nancy, France*
¶ *Université de Lorraine, UMR7365 IMoPA, CNRS, BioPole, Nancy, France*

ARTICLE INFO

Article history:
Received 13 July 2022
Accepted 30 December 2022

Keywords:
Chondrocytes
Collagen type I
5.8S rRNA
Ribosome
Preferential translation
rRNA epitranscriptomic regulation

SUMMARY

Objective: Osteoarthritis-related cartilage extracellular matrix remodeling is dependent on changes in chondrocyte protein expression. Yet, the role of ribosomes in chondrocyte translation regulation is unknown. In this exploratory study, we investigated ribosomal RNA (rRNA) epitranscriptomic-based ribosome heterogeneity in human articular chondrocytes and its relevance for osteoarthritis.
Methods: Sequencing-based rRNA 2′-O-methylation profiling analysis (RiboMethSeq) was performed on non-OA primary human articular chondrocytes ($n = 5$) exposed for 14 days to osteoarthritic synovial fluid (14 donors, pooled, 20% v/v). The SW1353 *SNORD71* KO cell pool was generated using Lenti-CRISPRv2/Cas9. The mode of translation initiation and fidelity were determined by dual-luciferase reporters. The cellular proteome was analyzed by LC–MS/MS and collagen type I protein expression was evaluated by immunoblotting. Loading of *COL1A1* mRNA into polysomes was determined by sucrose gradient ultracentrifugation and fractionation.
Results: We discovered that osteoarthritic synovial fluid instigates site-specific changes in the rRNA 2′-O-me profile of primary human articular chondrocytes. We identified five sites with differential 2′-O-me levels. The 2′-O-me status of 5.8S-U14 (one of identified differential 2′-O-me sites; decreased by 7.7%, 95% CI [0.9–14.5%]) was targeted by depleting the level of its guide snoRNA *SNORD71* (50% decrease, 95% CI [33–64%]). This resulted in an altered ribosome translation modus (e.g., CrPV IRES, FC 3, 95% CI [2.2 –4.1]) and promoted translation of *COL1A1* mRNA which led to increased levels of COL1A1 protein (FC 1.7, 95% CI [1.3–2.0]).
Conclusions: Our data identify a novel concept suggesting that articular chondrocytes employ rRNA epitranscriptomic mechanisms in osteoarthritis development.

Introduction

Translation and its precise regulation are critical for chondrocytes and articular cartilage homeostasis. Remodeling and degeneration of articular cartilage extracellular matrix (ECM) are hallmarks of OA, and they are fueled by alterations in chondrocyte protein expression programs[1]. However, ribosomes, cellular nanomachines that catalyze protein synthesis, have been largely overlooked in OA research. Understanding of ribosomes and their diverse roles in protein translation has grown significantly over the last decade. As a result, ribosomes, which were once considered homogenous in their composition and passive and non-selective in mRNA translation, are now recognized as heterogeneous and actively participating in translation regulation[2]. A single human cell contains millions of ribosomes consisting of four ribosomal RNAs (rRNAs; 18S, 5.8S, 28S, and 5S) and up to 80 ribosomal proteins (RPs) assembled into small (SSU; 40S) and large ribosomal subunits (LSU;

* Address correspondence and reprint requests to: T.J.M. Welting, Laboratory for Experimental Orthopedics, Department of Orthopedic Surgery, Maastricht University, Maastricht, the Netherlands.
E-mail address: t.welting@maastrichtuniversity.nl (T.J.M. Welting).

https://doi.org/10.1016/j.joca.2022.12.010

60S)[3]. The polypeptide-generating catalytic properties of the ribosome are executed by rRNAs[4] that are post-transcriptionally modified (PTM)[5,6]. 2′-O-methylation and pseudouridylation (ψ) are the most abundant rRNA modifications[6]. They represent a major source of ribosome heterogeneity and affect rRNA stability, ribosome biogenesis and function[2]. To date, over 100 2′-O-methylation sites have been identified in human rRNAs[7]. Box C/D snoRNAs (SNORDs) site-directionally guide 2′-O-me modifications of specific rRNA nucleotides by base-pairing with target rRNA. Subsequently, the methyltransferase fibrillarin (FBL) catalyzes the transfer of a methyl group to the 2′-hydroxyl group of target rRNA ribose[8]. 2′-O-me-based ribosome heterogeneity has been documented in the development and diseases such as cancer and dyskeratosis congenita[9]. Moreover, a recent study provided a functional link between cancer-specific 2′-O-me ribosome heterogeneity, translation of specific mRNAs, and pathological changes in cellular phenotype[10].

In this study, we investigated whether 2′-O-me-based ribosome heterogeneity of human articular chondrocytes (HACs) is modulated by OA synovial fluid (OA-SF), and we examined its functional relevance for OA pathobiology.

Materials and methods

Translation modus and fidelity assays

To investigate cellular translation characteristics, we used dual-luciferase reporters and probed cap-independent IRES-mediated translation initiation and translation fidelity (stop codon skipping and frameshift). Transfections were performed using the Fugene6 Transfection Reagent (Promega, E2691). Dual-luciferase reporters (DLRs) were gifts from S. R. Thompson and J. Dinman (Table S1). Firefly and Renilla luciferase activity were measured (48 h–72 h post-transfection) using the Dual-Luciferase® Reporter Assay System (Promega, E1910) and Tristar2 LB942 (Berthold Technologies). Raw RLU values are listed in Table S2[11]. β-galactosidase activity in lysates of cells co-transfected with a lacZ plasmid was measured by β-Gal Assay Kit (Invitrogen, K1455-01). Data were analyzed by a Mann–Whitney U test.

Synovial fluid collection

SF collection was approved by the Medical Ethics Committee (METC) from the Maastricht University Medical Center (2017-0183). SF samples were collected from patients ($n = 14$; average age 67.1 ± 5.5 years) suffering from knee OA undergoing total knee replacement surgery. Informed consent was acquired following Dutch medical ethical guidelines.

Human articular chondrocytes isolation and culture

Non-OA primary HACs were isolated from resected pieces of the knee of individuals undergoing arthroscopy, anterior cruciate ligament repair or osteochondritis dissecans surgery ($n = 5$; average age 19 years). Material collection and use were approved by the METC of Maastricht University Medical Center (2017-0183), and informed consent was acquired. Cartilage was digested overnight at 37°C in a type II collagenase (Gibco Life Technologies, 17101-015) (300 U/ml) in DMEM/F12 HEPES (Gibco Life Technologies, 31330038) with 1% Antibiotic-Antimycotic (A–A; Gibco Life Technologies, 15240-062). Chondrocytes were isolated by passing the digested cartilage over a 70-μm cell strainer (Greiner Bio-One, 542070). Cells were cultured in DMEM/F-12 low glucose with GlutaMAX (Gibco Life Technologies, 31331-093), 10% fetal calf serum (FCS; Sigma-Aldrich, F7524), 1% A–A (Gibco Life Technologies, 15240-062), 1% nonessential amino acids (NEAA; Gibco Life Technologies, 11140-035) at 37°C in a humidified atmosphere containing 5% CO_2. After reaching confluency, HACs were passaged 1:2 until passage 2. Non-OA HACs of five individual donors were plated in 24-well plates at 30,000 cells/cm^2 and exposed to 20% (v/v) OA-SF (pool of 14 patients to minimize the interpatient variability, equal volume ratios), or 20% (v/v) 0.9% NaCl in DMEM/F-12 GlutaMAX, 10% FCS, 1% A–A and 1% NEAA for 14 days. Culture medium was refreshed every other day.

RNA isolation and RiboMethSeq

Total RNA was isolated using the RNeasy Plus Mini Kit (Qiagen,74134). RNA quality was determined with a 2100 Bioanalyzer (Agilent) and RNA 6000 Nano Kit (Agilent, 5067-1511). RiboMethSeq of rRNAs was performed as previously described[12,13]. Briefly, ~100 ng of total RNA was fragmented by alkaline hydrolysis and the fragments were end-repaired. The NEBNext Small RNA kit (NEB, E7330S) was used to prepare the library. Libraries were multiplexed and sequenced using Illumina HiSeq 1000.

Bioinformatics pipeline was performed as previously described[13]. The MethLevel represents a fraction of rRNAs modified at a given nucleotide in the rRNA population normalized to an *in vitro* synthesized non-modified control rRNA transcript, MethLevel of 1 corresponds to a fully 2′-O-methylated position. RNA sequencing data are deposited in the ArrayExpress (E-MTAB-11469, E-MTAB-11470).

Visualization of the human ribosome and mapping of 5.8S-U14

5.8S-U14 site was visualized using PyMOL software and the three-dimensional structure of the human 80S ribosome was obtained from the Protein Data Bank (PDB ID: 6QZP)[14,15].

CRISPR/Cas9 targeting

A second-generation lentiviral production system was used. LentiCRISPR v2 was a gift from Dr. Feng Zhang (Addgene plasmid #52961; http://n2t.net/addgene:52961; RRID: Addgene_52961)[16]. Plasmids pCMVR8.74 and pMD2.G were gifts from Dr. Didier Trono (Addgene plasmid #22036; http://n2t.net/addgene:22036; RRID:Addgene_22036; Addgene plasmid #12259; http://n2t.net/addgene:12259; RRID:Addgene_12259). *SNORD71* targeting sgRNA sequences were based on a previous publication[17], annealed and cloned into LentiCRISPRv2 using BsmBI overhangs. LentiCRISPRv2 with sgRNAs targeting GFP was used as a CRISPR control[18,19]. All plasmids were sequence-verified. Lentiviruses were produced by transfection of HEK293T cells with transfer and production plasmid DNAs in equimolar ratios using polyethylenimine (PEI, PEI/DNA ratio 2.5:1; Polysciences, 07923966-2). Viruses were harvested and concentrated with the Lenti-X Concentrator (Takara, 631232). Viral titers were determined using p24 ELISA (Fujirebio, 80563). Lentiviral transductions were performed in SW1353 using MOI (multiplicity of infection) of 1 in presence of polybrene (Sigma-Aldrich, H9268). Twenty-four hours later cells were selected using puromycin (Sigma-Aldrich, P8833). In all experiments, SW1353 (ATCC, HTB-94) were cultured in DMEM/F-12 low glucose with GlutaMAX (Gibco Life Technologies, 31331-093) with 10% FCS (Sigma-Aldrich, F7524), 1% A–A (Gibco Life Technologies, 15240-062) and HEK293T (ATCC, CRL-3216) were cultured in DMEM high glucose medium (Gibco Life Technologies, 41966029), 10% FCS (Sigma-Aldrich, F7524), 1% A–A (Gibco Life Technologies, 15240-062), 1% sodium pyruvate (Gibco Life Technologies, 11360070) at 37°C in a humidified atmosphere and 5% CO_2 at 37°C in a humidified atmosphere and 5% CO_2.

DNA isolation and surveyor assay

To confirm the successful targeting of DNA with CRISPR/Cas9, genomic DNA (gDNA) was isolated using the DNeasy Blood & Tissue Kit (Qiagen, 69504). The target region was amplified by PCR from 200 ng of gDNA using the high-fidelity Phusion polymerase (Thermo Scientific, F530L) and PCR primers spanning the genomic sgRNA target sites. PCR amplicons were purified and concentrated using the MinElute PCR Purification Kit (Qiagen, 28004). For the Surveyor Mutation Detection Assay (IDT, 706020), 300 ng of amplified DNA was hybridized and digested by Surveyor Nuclease S for 60 min at 42°C. Digestion fragments were separated on 1.5% agarose gel and detected using ethidium bromide with a Chemidoc MP imaging system (Bio-Rad).

RT-qPCR

Total RNA (600 ng) was reverse transcribed using random hexamers (Promega, C1181). A quantitative polymerase chain reaction (qPCR) was performed using Takyon™ No Rox SYBR Master Mix blue dTTP (Eurogentec, UF-NSMT-B0710), cDNA (6 ng), forward and reverse primers (300 nM) and protocol: 50°C for 2 min, denaturation at 95°C for 10 min, followed by 40 cycles of amplification (15 s 95°C and 1 min 60°C) followed by a melting curve (Bio-Rad CFX96 Real-Time PCR Detection System). Data were analyzed using the standard curve method (Bio-Rad CFX Manager Software version 1.1). Relative quantification of target gene expression was normalized to a reference gene. Gene expression data were log-transformed for statistical analyses and presented as fold change. Primer sequences are listed in Table S1.

DNA measurements

Cells were plated subconfluently and cultured in the presence of ribosome-targeting antibiotics: emetine (EMT; Sigma-Aldrich, SMB01061), CHX (Sigma-Aldrich, C1988), anisomycin (ANS; Sigma-Aldrich, A9789), or fusidic acid (FA; Sigma-Aldrich, F0756). Cells were stained with 0.1% crystal violet (Sigma-Aldrich, C-3886) in 200 mM boric acid (pH 9.0) (Sigma-Aldrich, B7901). Bound dye was solubilized by 10% acetic acid (VWR, 20102292) and optical density was measured at 590 nm using a Multiskan FC Microplate Photometer (Thermo Scientific). In transfection experiments, the DNA content of the well was measured by SybrGreen (Life Technologies, S7563) using Tristar2 LB942 (Berthold Technologies). Fold change data were analyzed by Mann–Whitney U test (each time/concentration tested individually).

Total protein synthesis

SNORD71 KO and CRISPR control SW1353 cells pools were cultured in methionine and cysteine-free medium supplemented with EasyTag™ EXPRESS 35S Protein Labeling Mix (25 μCi/ml; PerkinElmer, NEG772002MC). After 30 min incubation, cells were harvested by scraping in Radioimmunoprecipitation assay (RIPA). The radioactive signal was measured with Tri-Carb 2910 TR scintillation counter (PerkinElmer). Data were normalized to total protein content of the well measured by bicinchoninic acid (BCA) Assay (Sigma-Aldrich, 71285-3).

Label-free mass spectrometry cellular proteomics

SNORD71 KO and CRISPR control SW1353 cell pools at 70–80% confluency were harvested from quadruplicate wells of a 6-well plate in 25 mM ammonium bicarbonate buffer (Sigma-Aldrich, 09830) with 7.5U of Benzonase nuclease (Merck Millipore, 70664-3) and protease inhibitor (Sigma-Aldrich, 11836170001). Samples were sonicated and centrifuged and stored at −80°C. Protein sample preparation and label-free liquid chromatography–tandem mass spectrometry (LC–MS/MS) were performed as previously described[20]. Briefly, proteolytic digestion was undertaken on 10 μg protein. In-solution tryptic digestion of protein samples was carried out following sequential reduction and alkylation in 3 mM DTT (60°C for 10 min) and then 9 mM iodoacetamide (30 min in the dark at room temperature) with trypsin/LysC at a ratio of 1:50 protein: trypsin ratio overnight at 37°C. Samples were run in a single batch following randomization for loading on LC–MS/MS analysis using an Ultimate 3,000 Nanosystem (Dionex, ThermoFisher Scientific) online to a Q-Exactive Quadrupole-Orbitrap instrument (Thermo Scientific)[21]. Progenesis QI software (V4, Waters) was used for label-free quantification[22]. The retention times of samples were aligned after the selection of a reference sample. Feature picking used the top three spectra for each feature. These were utilized for peptide identification with a locally implemented Mascot server (Matrix Science) in the UniHuman Reviewed database. Search parameters were as follows: enzyme; trypsin, peptide mass tolerances 10 ppm, fragment mass tolerance of 0.01 Da, 1+, 2+, and 3+ ions, with carbamidomethyl cysteine as a fixed modification and methionine oxidation as a variable modification with a false discovery rate (FDR) of 1%. Only unique peptides were used for quantification. Protein expressions were log-transformed for statistical analyses (one-way analysis of variance (ANOVA)) and are presented as fold change. All peptides (with a significant Mascot score >23 and FDR <0.05) of an identified protein were included, and the protein *P*-value (one-way analysis of variance) was then performed on the sum of the normalized abundances for all runs. Proteins with q-value < 0.05, and FC ≥ 1.5 were considered to be differentially expressed (DE). Proteomic data were deposited in the PRIDE ProteomeXchange (PXD032752). Ingenuity Pathway Analysis (IPA) (Qiagen) was used for the functional analysis of DE proteins[23].

Immunoblotting

Chondrocytes were lysed in RIPA buffer (150 mM NaCl, 50 mM Tris–HCl, 5 mM EDTA, 0.5 mM DTT, 1% NP-40, 0.5% DOC, and 0.1% SDS) with protease inhibitor cocktail (Sigma-Aldrich, 11836170001). Samples were sonicated on ice using the Soniprep 150 (MSE) and spun (13.000 g, 4°C, 10 min). Protein concentration was determined using the BCA Protein Assay Kit (Abcam, ab102536). Equal amounts of the lysate (20 μg) were loaded and separated by SDS-PAGE using a 4–15% precast polyacrylamide gel (Bio-Rad, 4568084). Nitrocellulose membranes were blocked with Tris-buffered saline with 5% skimmed milk powder and 0.1% NP-40 and probed with primary antibodies: Anti-Collagen Type I (1:1000; Southern Biotech, 1310-01) and anti-GAPDH (1:5000; Fitzgerald, 10R-G109b). Bound primary antibodies were detected with horseradish peroxidase (HRP)-conjugated secondary antibodies (1:1000; Dako Agilent, P0260, P0449) and visualized using a chemiluminescent HRP substrate (Dako Agilent, K400311-2), ChemiDoc XRS$^+$ System (Bio-Rad) and Image LabSoftware (Bio-Rad). The relative quantitation of the signal corrected for the background and GAPDH was performed using Image LabSoftware (Bio-Rad).

Polysome profiling

To determine the translational activity of target genes, we separated ribosomal subunits, monosomes and polysomes by polysomal profiling. *SNORD71* KO and CRISPR control SW1353 cell pools at 70–80% confluency were pre-incubated with cycloheximide (CHX, 100 μg/ml, Sigma-Aldrich, C1988) for 20 min at 37°C, harvested by scraping in cold NaCl (0.9%) supplemented with CHX (100 μg/ml),

centrifuged at 1.100 rpm for 10 min and resuspended in polysome extraction buffer (20 mM Tris–HCl (pH7.5), 100 mM KCl, 5 mM $MgCl_2$, 0.5% NP-40), with CHX 100 μg/ml, protease inhibitor cocktail (Sigma-Aldrich, 11836170001) and recombinant RNasin (40 U/ml, Promega, N2515)[24]. Cytoplasmic extracts were centrifuged at 13.200 rpm at 4°C for 10 min. Linear sucrose gradients were prepared by layering 50% sucrose solution (0.5 M NaCl, 100 mM Tris–HCl (pH7.5), 50 mM $MgCl_2$, 50% sucrose) under a 10% sucrose solution (0.5 M NaCl, 100 mM Tris–HCl (pH7.5), 50 mM $MgCl_2$, 10% sucrose) in Open-Top Polyclear tubes (Senton, 7030), mixed by Gradient Master 108 (BioComp). Equal amounts of cytoplasmic extracts were loaded on the sucrose gradients and centrifuged at 39.000 rpm at 4°C for 1.5 h (SW 41 Ti rotor, Beckman-Coulter, 331362)[24]. Sucrose gradient fractions (24 fractions, 500 μl each) were separated using a Piston Gradient Fractionator (BioComp) coupled to a Fraction Collector (Gilson). Optical density at 260 nm was measured continuously (Piston Gradient Fractionator, Triax Flow Cell software). Equal volumes of 8 M guanidine-HCl (Sigma-Aldrich, G4505) and FLUC RNA spike-in control (1 ng/fraction; Promega, L4561) was added to each fraction. RNA was precipitated with 3 M NaAc (pH 5.2) (VWR, 27653.260) and isolated using the RNeasy Plus Mini Kit (Qiagen,74134). Equal volumes of RNA were reverse transcribed and measured by qPCR as described earlier. Relative expression and the percentage distribution of the mRNAs across the gradient were calculated by the ΔCT method[24] using 28S rRNA as a reference gene and normalized to the signal from spiked FLUC.

Statistical testing

All statistical analyses were performed with Graphpad Prism version 5.0.1. (California, USA). Normal distribution of the data was tested or assumed (as indicated in corresponding Figure legends). Differences between the two groups were determined by a two-tailed unpaired *t*-test, and two paired groups were assessed by a two-tailed paired *t*-test. Differences between two groups with non-normal distribution were evaluated by the Mann–Whitney U test. Detailed descriptions of the employed statistics are specified in the Figure legends. Data are presented with individual dot plots with a mean ± 95% confidence interval and are considered statistically significant when $P < 0.05$.

Results

Osteoarthritic synovial fluid affects translation initiation and fidelity

First, we tested the capacity of OA-SF to affect chondrocyte translation characteristics. Using SW1353 as a model for

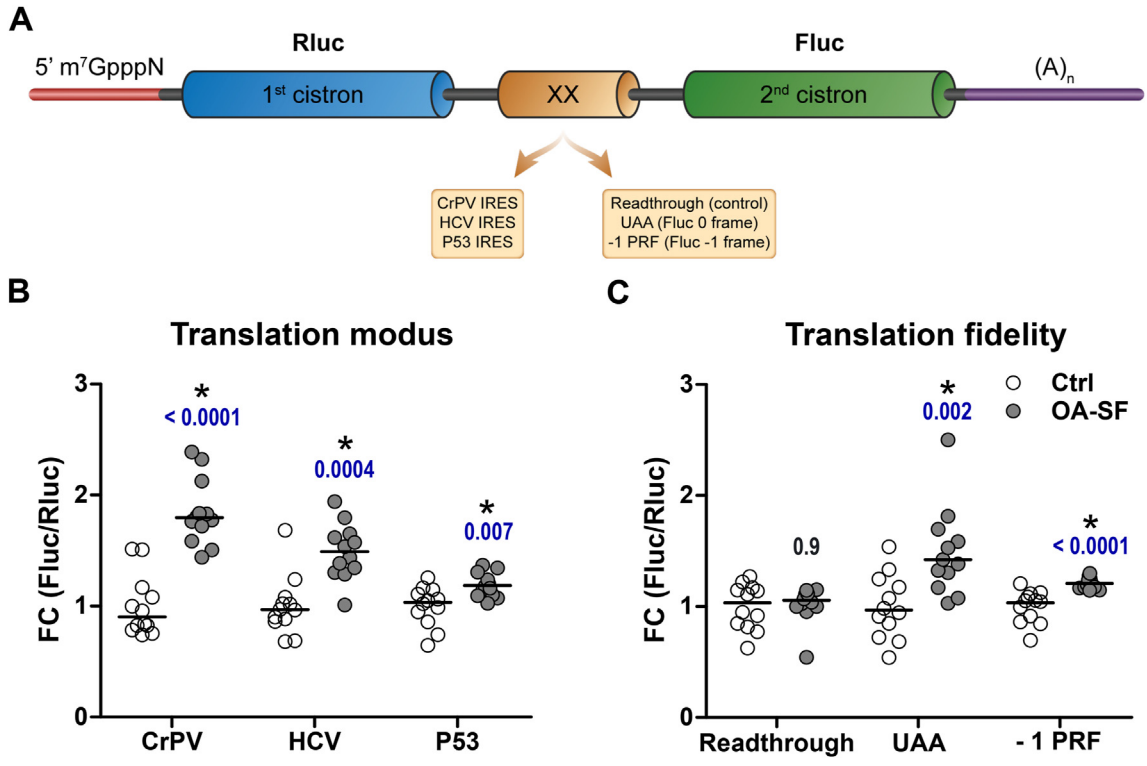

Fig. 1

Osteoarthritis and Cartilage

Osteoarthritic synovial fluid increases translation from IRES elements and compromises translation fidelity (A) Schematic illustrating the transcript of the dual-luciferase reporters used to measure the mode of translation initiation from IRES elements (CrPV, HCV and P53) and translation fidelity (UAA – stop codon skipping, and –1 PRF – frameshift). (B–C) The effect of the osteoarthritic microenvironment on translation modus and fidelity. SW1353 cells were transfected with DLRs and stimulated with end-stage osteoarthritic synovial fluid (OA-SF; 20% (v/v), pool of 14 donors) for 48 h. Fluc/Rluc data ($n = 12$; each data point representing an individual transfection) are corrected for the DNA content of the well. Data are plotted as fold change to Control. Statistical significance was assessed by the Mann–Whitney U test.

chondrocytic cells and dual-luciferase reporter assays we probed cap-independent translation initiation and translation fidelity [Fig. 1(A)]. OA-SF treated cells demonstrated increased capacity to initiate translation from tested IRES elements, CrPV (FC 1.8, 95% CI [1.6–2.0]), HCV (FC 1.5, 95% CI [1.3–1.7]), and P53 (FC 1.2, 95% CI [1.1–3.2]) [Fig. 1(B)]. In terms of translation fidelity, OA-SF treatment increased incidence of stop codon skipping (UAA in 0 frame, FC 1.5, 95% CI [1.2–1.7) and −1 frameshift (HIV-1 PRF, FC 1.2, 95% CI [1.1–1.3]) [Fig. 1(C)]. These results demonstrate that OA-SF as an OA-relevant microenvironment affects several aspects of protein translation in SW1353 cells.

Osteoarthritic synovial fluid instigates site-specific changes in chondrocyte rRNA 2′-O-me profiles

We previously described an OA *in vitro* model in which prolonged exposure of non-OA HACs to OA-SF drove chondrocytes towards a fibrochondrocyte phenotype[25]. In the current study, we used OA-SF and five individual non-OA HAC donors to investigate OA-SF-dependent rRNA 2′-O-me heterogeneity in chondrocytes [Fig. 2(A)]. Using a sequencing-based rRNA 2′-O-methylation profiling method RiboMethSeq[13], we identified 109 rRNA 2′-O-me sites (Fig. S1 and Table S3). By comparing the rRNA 2′-O-me profiles of OA-SF treated and control chondrocytes, we identified five sites with differential OA-dependent 2′-O-me levels: 18S-G1447, 5.8S-U14, 28S-A3739, 28S-A3846 and 28S-U4590 (Fig. 2(B); 18S-G1447 10.4% decrease, 95% CI [5.9–14.8], 5.8S-U14 7.7% decrease, 95% CI [0.9–14.5], 28S-A3739 5.7% decrease, 95% CI [3.3–7.9], 28S-A3846 10.4% increase, 95% CI [1.5–19.3], 28S-U4590 6.2% increase, 95% CI [1.4–10.9]). One of the identified sites, 5.8S-U14, is located within the functionally important region of the ribosome, the 28S-5.8S rRNA junction [Fig. 2(C)]. Its methylation status affects the conformational state of 5.8S and its interaction with 28S[26]. Moreover, differential 2′-O-me levels of 5.8S-U14 have been reported in various tissues and cancer cells[7,27–29], suggesting the functional relevance of this PTM. Therefore, we focused on this particular rRNA PTM site in our follow-up work.

Depletion of SNORD71 reduces 5.8S-U14 2′-O-me levels, affects translation initiation, fidelity, and ribosome translocation

The 2′-O-me of 5.8S-U14 (5.8S-Um14) is guided by an intron-encoded box C/D small nucleolar RNA (snoRNA) SNORD71 [Fig. 3(A)][30]. To impact the 2′-O-me status of 5.8S-U14, we generated a *SNORD71* knockout (*KO*) SW1353 cell pool using CRISPR/Cas9 gene editing. Two sgRNAs were used simultaneously to delete a segment of the *SNORD71* gene including the 5.8S-U14-complementary sequence [Fig. 3(B)]. The efficiency of the CRISPR/

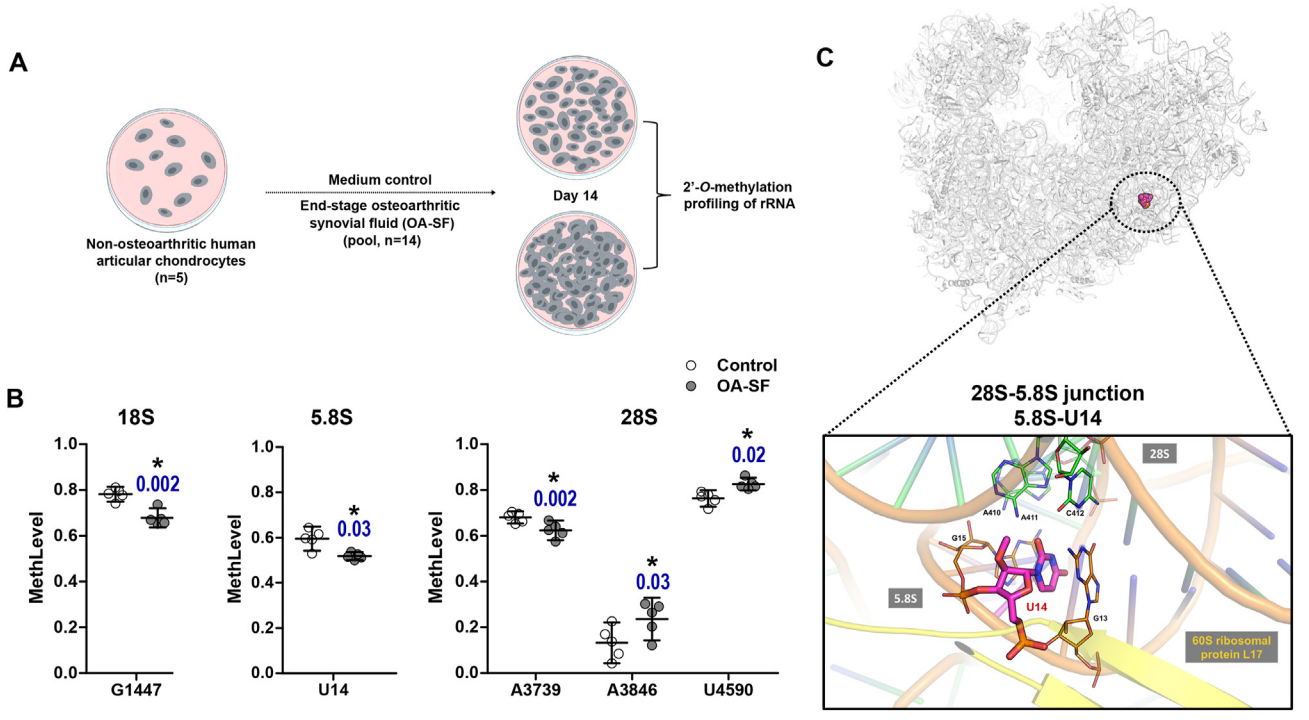

Fig. 2

Osteoarthritis and Cartilage

Osteoarthritic synovial fluid induces site-specific changes in 2′-O-methylation of ribosomal RNAs in chondrocytes. (A) Scheme of the experimental set-up. Human non-OA HACs (5 individual donors) were cultured either in the presence of OA-SF (20% (v/v), pool of 14 donors) or in a normal culture medium and were refreshed every other day. After 14 days of culture, RNA was isolated for 2′-O-methylation profiling of ribosomal RNAs. (B) Differentially 2′-O-methylated rRNA nucleotides. Statistical significance was assessed by paired *t*-test with the assumption of normal distribution of the data. Full 2′-O-me rRNA profiles are shown in Fig. S1. (C) Location of 5.8S-U14 within the 28S-5.8S junction of the human ribosome.

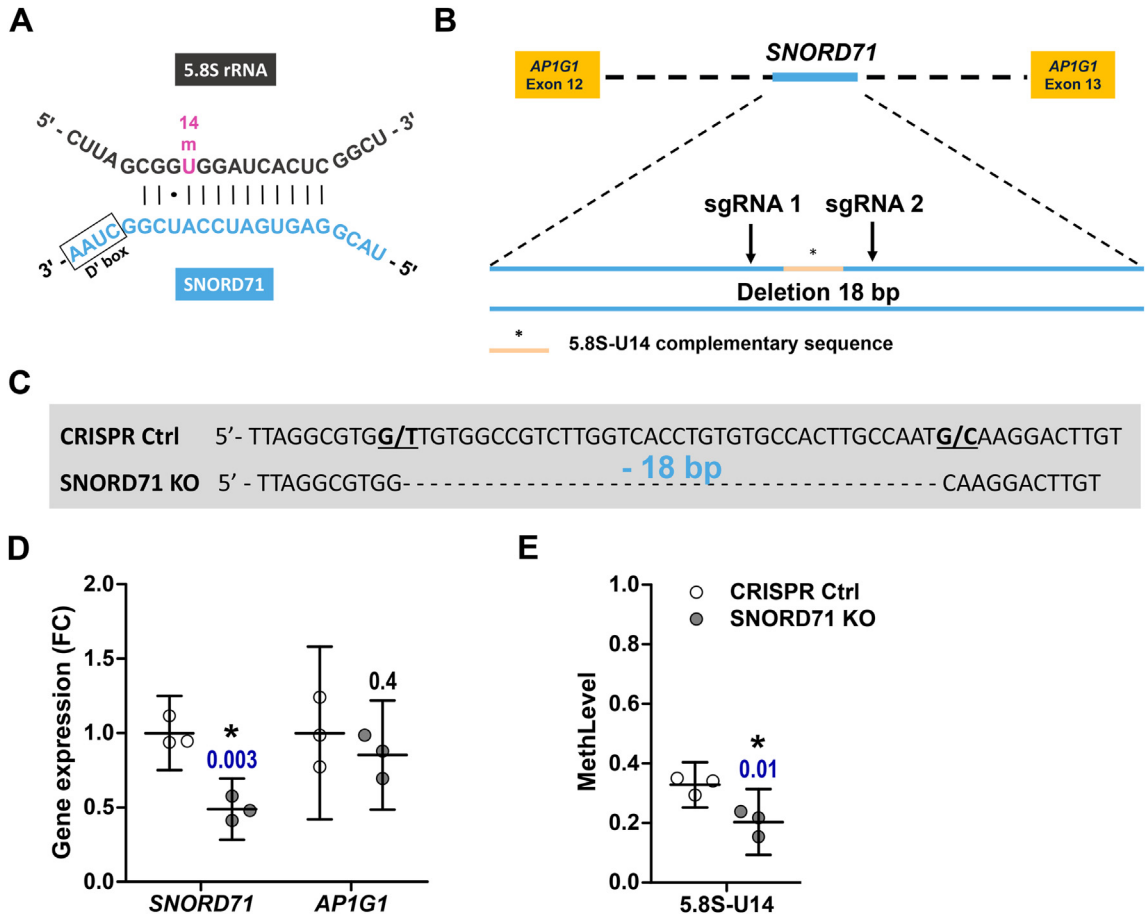

Fig. 3

Osteoarthritis and Cartilage

CRISPR/Cas9-mediated *SNORD71* depletion reduces 5.8S-U14 2′-O-methylation levels. (A) The box C/D snoRNA SNORD71 is predicted to direct 2′-O-me of nucleotide U14 of 5.8S rRNA[30,32] (B) A scheme of the double sgRNA CRISPR/Cas9-mediated approach to generate *SNORD71* knockout SW1353 cell pool. Top: Exons of the host gene *AP1G1* flanking the intron-encoded *SNORD71*. Bottom: *SNORD71* sequence with the 5.8S-U14 complementary sequence flanked by sgRNA1 and sgRNA2 target cleavage sites. Double lentiviral transduction with sgRNA1 and sgRNA2 was performed in SW1353 cells. CRISPR/Cas9-treated SW1353 cells with sgRNAs targeting GFP were used as a control (CRISPR Ctrl). (C) Schematic of the genomic modification in the cell population assessed by sequencing. SgRNA1 and sgRNA2 cleavage sites are indicated in bold and a slash respectively. (D) Expression levels of *SNORD71* and its host gene *AP1G1* in CRISPR Ctrl and *SNORD71*-depleted SW1353 cell pools measured by RT-qPCR. Expression levels were normalized to the reference gene (*PPIA*) expression and are plotted as fold change of original values. Data ($n = 3$) were analyzed by unpaired *t*-test with the assumption of normal distribution of the data. (E) 2′-O-me levels of 5.8S-U14 in CRISPR Ctrl and *SNORD71*-depleted SW1353 cells were measured by RiboMethSeq ($n = 3$) and analyzed by unpaired ***t***-test with the assumption of normal distribution.

Cas9-mediated *SNORD71* editing in the KO SW1353 cell pool was confirmed using the surveyor nuclease assay (Fig. S2). DNA sequencing confirmed an overall 18 bp deletion in the *SNORD71* gene [Fig. 3(C)] in the SNORD71 KO SW1353 cell population. We found a 50% decrease in *SNORD71* expression (FC 0.5, 95% CI [0.3–0.6]) without any apparent effect on SNORD71 host gene expression (*AP1G1*, 95% CI [−0.3 to 0.8] Fig. 3(D)). Moreover, we measured a significant decrease in 5.8S-Um14 levels in *SNORD71*-depleted SW1353 cells (Fig. 3(E); 12% difference, 95% CI [3.8–21.2]) and additional changes in modification level of two additional rRNA nucleotides (Tables S4–5). Next, we proceeded with evaluating the effects of *SNORD71* depletion on ribosome function of SW1353 cells. *SNORD71* depletion did not affect SW1353 proliferation (Fig. 4(A); 95% CI [0.8–1.0] (Day 0), [0.3–1.2] (Day 2), [0.5–1.4] (Day 4), and [0.1–4.8] (Day 6)). We also did not notice any differences in global protein translation [Fig. 4(B)], or global polysomal distribution [Fig. 4(C)]. The cap-over IRES-mediated translation initiation revealed an increased capacity of *SNORD71*-depleted SW1353 cells to initiate translation from three distinct IRES elements (Fig. 4(D); CrPV (FC 3, 95% CI [2.2–4.1]), HCV (FC 3.7, 95% CI [1.8–5.9]) and P53 (FC 4.4, 95% CI [1.8–7.7]). Translation accuracy was also affected, as evidenced by a greater incidence of stop-codon readthrough (FC 4.4, 95% CI [1.2–8.8]), as well as defective reading frame maintenance (FC 2, 95% CI

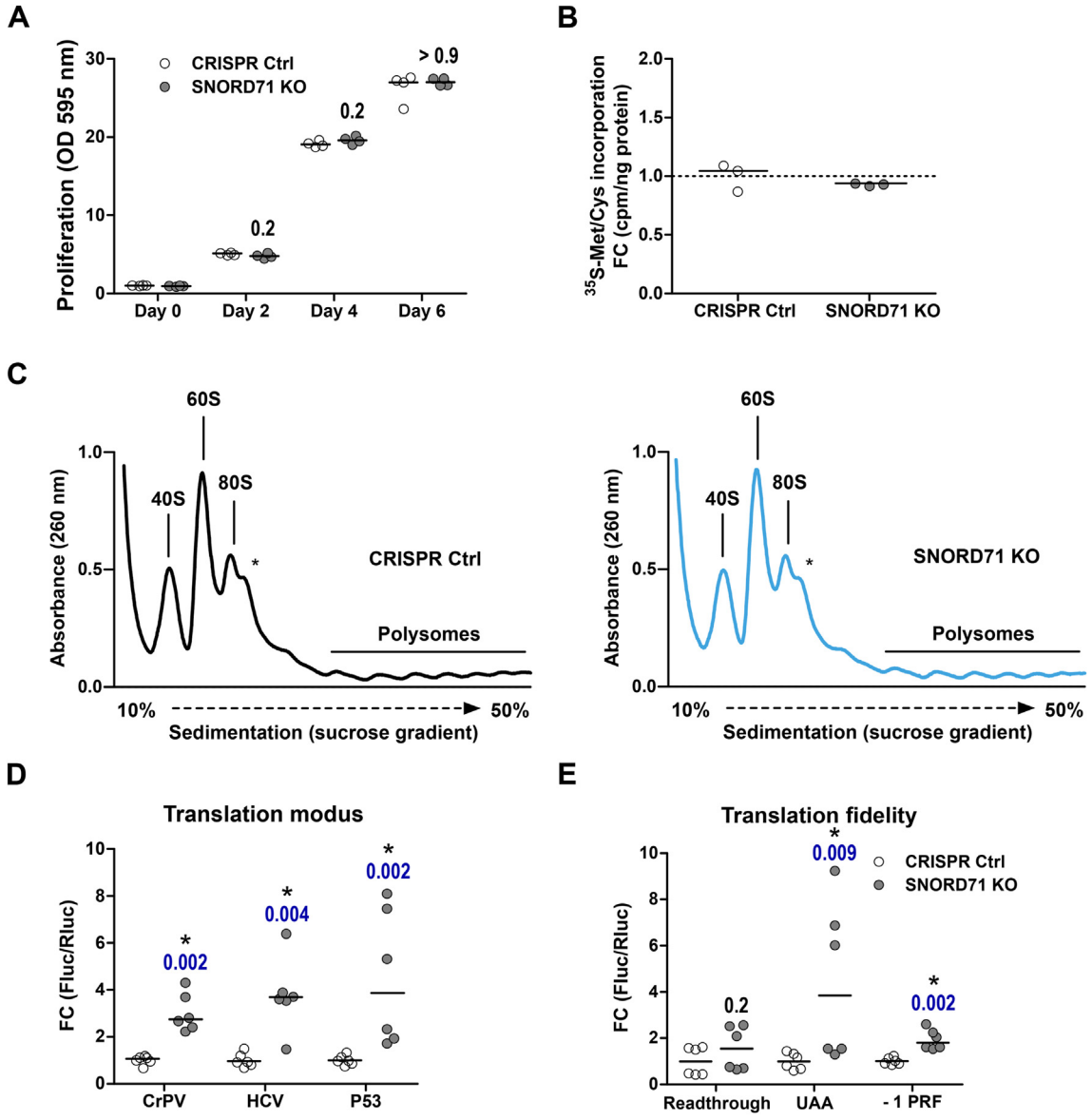

Fig. 4

Osteoarthritis and Cartilage

Depletion of *SNORD71* increases IRES/cap translation and reduces translation fidelity (A) Proliferation rate of CRISPR Ctrl and *SNORD71*-depleted SW1353 cells measured by crystal violet staining at day 0–6. Data ($n = 4$) are presented as fold change to Day 0. Data were analyzed by the Mann–Whitney U test. (B) Translation capacity of *SNORD71*-depleted SW1353 cells measured by [^{35}S]methionine/cysteine incorporation and normalized for protein content of the well. Data ($n = 3$) are presented as fold change to CRISPR control. (C) Polysome profiles of CRISPR control and *SNORD71*-depleted SW1353 cells. The asterisk indicates halfmer monosomes[33]. (D–E) The effect of *SNORD71* depletion on translation modus and fidelity. Fluc/Rluc data ($n = 6$; each datapoint represents a single transfection of either CRISPR control or *SNORD71*-depleted SW1353 cells) are corrected for the β-galactosidase activity of the co-transfected lacZ gene and plotted as fold change to CRISPR control. Data were analyzed by the Mann–Whitney U test.

[1.5–2.4]) [Fig. 4(E)]. To further probe for alterations in ribosome function, we tested a series of ribosome-targeting antibiotics that act on ribosomal subunits (EMT: 40S; CHX, ANS, FA: 60S) and critical steps of protein translation, such as translocation (EMT, CHX, FA) or aminoacyl–tRNA binding (ANS) (Fig. 5)[31]. *SNORD71*-depleted SW1353 pools were more sensitive to EMT (10 % more inhibition at 5 ng/ml, 95% CI [2.8–14.5], 11 % more inhibition at 10 ng/ml, 95% CI [4.5–18.2]), and CHX (7 % more inhibition at 0.64 μg/ml, 95% CI [5.6–8.4], 6 % more inhibition at 1.28 μg/ml, 95% CI [3.1–7.4]), but not to FA (1.9 % more inhibition at 40 μg/ml, 95% CI [−6.4 to 2.5], 1.5% less inhibition at 80 μg/ml 95% CI of [−0.14 to 3.9]). Data collectively suggest a role of *SNORD71* depletion and 5.8S-Um14 status on multiple aspects of translation of chondrocytic cells.

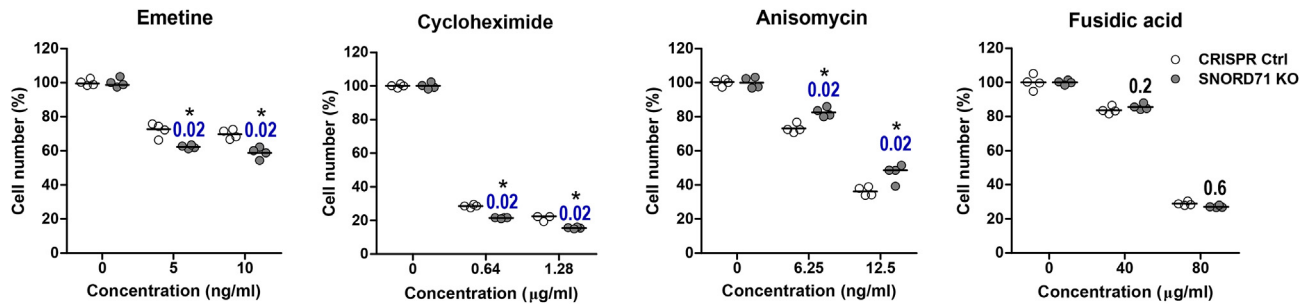

Fig. 5

Osteoarthritis and Cartilage

SNORD71 depletion affects the sensitivity of cells to ribosome-targeting antibiotics. Cell sensitivity to translation inhibitors emetine (EMT), cycloheximide (CHX), anisomycin (ANS), and fusidic acid (FA) was assessed by calculating the percentage of surviving cells (CRISPR Ctrl and *SNORD71*-depleted SW1353 cell pools) on day 6 of culture.EMT and CHX bind to the E-site of the 40S and the 60S ribosomal subunit respectively[31,34]. ANS binds to the A-site of 60S and destabilizes aminoacyl–tRNA binding[31]. FA targets ribosome-bound elongation factor 2 (EF-2), thus affecting translocation as well as ribosome recycling[35]. The data ($n = 4$) were assessed by the Mann–Whitney U test.

SNORD71 depletion increases protein expression of the fibrochondrocyte protein COL1A1

To assess the effects of *SNORD71* depletion on specific protein expression, we determined the cellular proteome of *SNORD71*-depleted SW1353. A total of 2929 proteins were detected and 334 proteins were differentially expressed (DE; FC > 1.5, q value < 0.05) in *SNORD71*-depleted SW1353 compared to CRISPR controls (Fig. 6(A), Table S6; 173 up, 161 downregulated). Several transcription (e.g., POLR1B, POLR2H, POLR2K, GTF2E2) and translation factors (e.g., EEF1A2, EIF3I, EIF3G, EIF1AD, CTIF) were among the upregulated proteins. Interestingly, EIF3G plays a role in HCV IRES recognition and translation initiation[18], and EEF1A2 is an activator of the Utrophin A IRES in muscle cells[19]. We compared these DE proteins with a collection of ribosome biogenesis factors[36], genes with putative cellular IRES elements[37] and IRES trans-acting factors (ITAFs)[38] (Fig. 6(A), Table S7). The comparison with ribosome biogenesis factors resulted in an overlap of 29 factors, the majority of which were upregulated in *SNORD71*-depleted SW1353. Ingenuity Pathway Analysis (IPA) (Table S8) identified P53 as the top upstream regulator (2.1E-29) and highlighted processes such as "RNA post-transcriptional modification (2.1E-29) and "Protein synthesis, degradation and post-translation modification" (1.09E-06 – 1.01E-22) in the "Disease and Bio Functions" category.

The only collagen upregulated in *SNORD71*-depleted SW1353 cells was the fibrotic collagen type I alpha 1 (COL1A1; FC 1.7, 95% CI [1.33–2.03]) [Fig. 6(B)]. Moreover, when we examined expression of collagen type I in OA-SF-stimulated HACs we observed a significant increase of its protein levels [Fig. 6(C)]. This implies that OA-SF, as well as *SNORD71* depletion, provoke OA-relevant changes in the chondrocyte proteome through the 5.8S-U14 2′-O-methylation status. To assess whether the increase in COL1A1 protein level was a result of transcriptional or translational regulation, we measured expression levels of total *COL1A1* as well as the distribution of *COL1A1* mRNA in polysome fractions from CRISPR control and *SNORD71*-depleted SW1353 cells. While we did not find a difference in the expression level of *COL1A1* between *SNORD71* KO and CRISPR control SW1353 cell pools (Fig. 6(D), 95% CI [0.8–1.04]), the relative abundance of *COL1A1* mRNA was higher in polysome fractions 8–23 of *SNORD71*-depleted SW1353 [Fig. 6(E)]. This suggests that the increased COL1A1 protein levels are a consequence of translational regulation and higher mRNA translation efficiency of the *COL1A1* transcript in *SNORD71*-depleted SW1353 cells. In conclusion, we showed that depletion of *SNORD71* in SW1353 cells leads to decreases 2′-O-me status of 5.8S-U14, affects the mode of ribosome translation initiation, compromises translation accuracy, and alters the cellular proteome. Moreover, the effects of *SNORD71* depletion on ribosome translation modus and fidelity, as well as the protein expression level of the OA fibrochondrocyte protein COL1A1, reproduced the results that we obtained in chondrocytes exposed to OA-SF as an osteoarthritis-relevant disease microenvironment.

Discussion

Cartiage ECM remodeling in osteoarthritis is driven by alterations in chondrocyte protein expression. However, changes in chondrocyte proteome and secretome cannot all be explained by transcriptional regulation alone[39]. Multiple studies reported an altered translation regulation in OA chondrocytes, mostly at the level of total translation rate[39]. In respect to other diseases, studies describing ribosome heterogeneity as a mechanism of translation regulation are emerging[2,40,41]. Recent development of sequencing-based rRNA 2′-O-methylation detection techniques enabled the generation of precise rRNA 2′-O-me profiles and allowed for mapping 2′-O-me-based ribosome heterogeneity in various physiological and pathophysiological conditions[9]. We used OA-SF to demonstrate that an OA-relevant microenvironment has the capacity to instigate site-specific changes in the rRNA 2′-O-me profiles of human primary chondrocytes, as well as induce IRES-mediated translation and compromise translation elongation and termination in chondrocytic SW1353 cells. Further analysis of one the OA-related differential rRNA 2′-O-me sites 5.8S-Um14 in SW1353 cells uncovered a link between epitranscriptomic ribosome heterogeneity and translation of the OA-relevant ECM protein COL1A1.

Human rRNA 2′-O-me sites can be classified as constitutive or variable. The group of constitutive modifications exhibits a stable level of modification in the cellular ribosome pool, are conserved among species, and cluster within functionally important regions of the ribosome (e.g., peptidyl transferase center, polypeptide exit

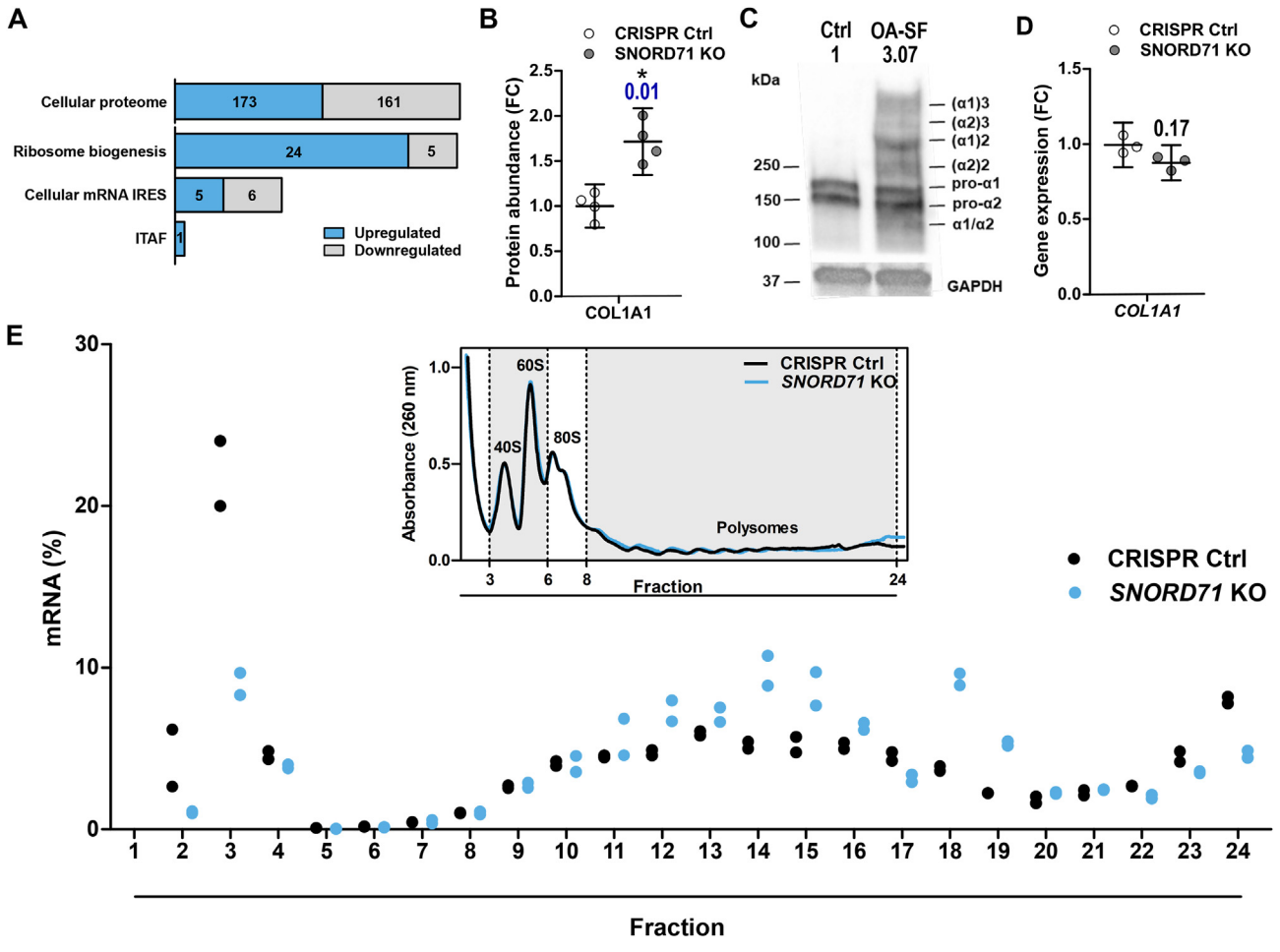

Fig. 6

Osteoarthritis and Cartilage

SNORD71 depletion affects the cellular proteome and increases translation of the fibrochondrocyte marker collagen type I. (A) The cellular proteome of *SNORD71*-depleted SW1353 cells was compared to CRISPR controls by LC–MS/MS and label-free quantification ($n = 4$). Statistical significance was assessed by one-way ANOVA (adjusted FDR, q, * <0.05). Normal distribution of the data was assumed. The blue and gray boxes represent proteins significantly up-or down-regulated in the *SNORD71* KO SW1353 cell pool. (B) Collagen type I alpha 1 protein abundance in *SNORD71* KO SW1353 cell pool measured by LC–MS/MS. Data ($n = 4$) are plotted as a fold change of original values to CRISPR Ctrl. (C) Immunoblot of collagen type I in primary human articular chondrocytes exposed to an OA-SF for 7 days. Results of the quantitation analysis are displayed as a fold change of the original values corrected for background and GAPDH to Ctrl condition. (D) Gene expression of *COL1A1* in *SNORD71* KO and CRISPR control SW1353 cell pool samples used for polysome fractionation measured by RT-qPCR. Expression levels were normalized to the reference gene (*PPIA*) expression. Data ($n = 3$) are plotted as fold change to CRISPR Ctrl and were analyzed by unpaired *t*-test with the assumption of normal distribution of data. (E) The relative distribution (percentage of total mRNA) of the *COL1A1* mRNA throughout the sucrose gradients of CRISPR control and *SNORD71* KO SW1353 cell pool.

tunnel and tRNA binding sites)[7]. On the other hand, variable rRNA 2′-O-me sites are present only in a subset of ribosomes and thus contribute to ribosome heterogeneity. They are less conserved throughout evolution and they are generally located at the periphery of the ribosome[7,9,27]. Variable sites are also more dynamically regulated and sensitive to various external and internal cellular conditions (e.g., hypoxia, P53 inactivation or depletion, MYC expression, NPM1, FBL, SNORD42, or SNORD45A abolishment)[9,10]. In accordance with this, all rRNA sites with differential 2′-O-me status in response to OA-SF (18S-G1447, 5.8S-U14, 28S-A3739, 28S-A3846 and 28S-U4590) belong to variable rRNA 2′-O-me sites[7,27]. Two of the identified OA-dependent rRNA 2′-O-me sites are situated within important functional regions of the ribosome. 28S-A3739 is located in the hairpin loop of helix 69 (H69) directly beside the inter-subunit rotation center and 5.8S-U14 is positioned in the 28S-5.8S junction where it interacts with ribosomal protein L17[26,27,42]. While 2′-O-me of 5.8S-U14 has not been reported in yeast, studies in mammals report sub-stoichiometric and differential 2′-O-me of 5.8S-U14 in cancer, differentiation, and various tissues[7,27–29]. Such dynamic regulation of 5.8S-Um14 suggests functional purposes and was therefore subjected to further analysis.

2′-O-me of 5.8S-U14 is predicted to be guided by the box C/D snoRNA SNORD71. We generated a *SNORD71* KO SW1353 cell pool with significantly decreased 5.8-Um14 levels, enabling us to investigate the roles of this PTM in translation. *SNORD71*-depleted SW1353 presented with increased sensitivity to translocation-targeting antibiotics, which is in alignment with previous studies reporting roles of 5.8S rRNA in the translocation step of elongation[43–45]. 5.8S rRNA molecules can adopt at least two distinct conformations depending on the modification status of 5.8S-U14[26]. *SNORD71*-depleted SW1353 did not exhibit any detectable impairment of global translation. However, we established that *SNORD71* depletion increases the capacity of SW1353 cells to initiate IRES-mediated translation, compromises translation fidelity, and provokes specific changes in the cellular proteome. Interestingly, one of the downregulated proteins was PWP1, a ribosome biogenesis factor previously reported to play a role in 5.8S rRNA folding and processing in the nucleolus[46]. More importantly, we measured increased levels of collagen type I alpha 1 (COL1A1) in *SNORD71*-depleted SW1353 cells and showed that it is a result of translational, rather than transcriptional regulation. COL1A1 is a key marker of the fibrochondrocyte subpopulation within osteoarthritic cartilage[47,48], and its protein expression strongly increases in primary HACs exposed to OA-SF *in vitro*[25]. These results are analogous to recent study in which depletion of *SNORD45C* and abolishment of 18S-Cm174, also did not affect global protein translation. Nevertheless, it affected translation efficiency of specific mRNAs which resulted in proteomic changes with consequences for cancer cellular phenotype[10]. Further analysis is warranted to establish how the 2′-O-methylation status of 5.8S-U14 regulates preferential translation of *COL1A1*. Nevertheless, our results suggest that 5.8S-Um14 status tunes translation of chondrocytes and contributes to OA pathobiology.

In this work, we have used pooled end-stage OA-SF as a model to investigate its effects on ribosome heterogeneity in primary HACs and ribosome function of chondrocytic SW1353 cells. The pooled approach was chosen to eliminate potential donor-specific variability and was also utilized in our previously published work[25,49,50]. In the current study, we did not compare the effects of non-OA and OA-SF. Recent data published by our group demonstrate critical differences between non-OA and OA-SF and reveal strong enrichment of OA-SF in inflammatory mediators, various growth factors and DAMPs with important consequences for chondrocyte signaling and phenotype[25,50]. In the future, a direct comparison of non-OA and OA HACs and cartilage explants would be of interest to broaden our research on ribosome heterogeneity and its functional consequences in OA.

A limitation of our study is the use of a *SNORD71* KO cell pool rather than generating single-cell clones with homozygous modification. However, this is a time efficient method that allowed us to perform follow-up experiments within a relatively short time frame and thus minimized likely selective pressure against KO cells such as reported in homozygous KO cell lines[51]. Despite using a KO cell pool, the level of residual 5.8S-Um14 in the population of *SNORD71*-depleted cells was only 20%. In fact, such residual modification level resembles the (patho)physiological situation more accurately than its complete ablation which would potentially be the case in *SNORD71* knockout cells. Reviewing the full rRNA 2′-O-me profiles of *SNORD71*-depleted SW1353 cells we noted a minor change in modification levels of two other rRNA nucleotides: 18S-C797 and 28S-A4560. Coordinated modification status of various rRNA sites without shared snoRNA has been reported recently[51], implying a complex regulation and compensatory or competitive relationships between individual PTMs[52].

The turnover of ribosomal RNAs (and ribosomes) is relatively slow compared to other RNA species, such as mRNAs[53,54]. Currently, no enzymes capable of “erasing” rRNA 2′-O-me have been identified. Therefore, it is tempting to contemplate the possibility that ribosomes with a specific rRNA 2′-O-me signature could be synthesized during the course of chronic disease such as OA and gradually promote its progression by preferential translation of OA-related mRNAs.

In conclusion, we present evidence that the osteoarthritic synovial fluid provokes site-specific changes in rRNA 2′-O-me profiles in primary HACs. Moreover, we discovered that rRNA 2′-O-me heterogeneity represents an epitranscriptomic regulatory mechanism that controls translation of specific osteoarthritis-relevant mRNAs in chondrocytes. This opens up a new area of therapeutic molecular targets for the treatment of osteoarthritis.

Data availability, accession numbers

RNA sequencing data are deposited in the ArrayExpress (E-MTAB-11469, E-MTAB-11470). Proteomic data are deposited in the PRIDE ProteomeXchange (PXD032752).

Author contribution statement

A.Ch., G.G.H. van den A., and T.J.M.W. performed study concept and design; A.Ch., G.G.H. van den A., B.A.C.H., A.C., D.A.M.S., K.W., M.J.P., V.M, Y.M., T.J.M.W. provided acquisition, analysis and interpretation of data, and statistical analysis; A.Ch., G.G.H. van den A., B.A.C.H., M.M.J.C., A.C., D.A.M.S., M.J.P, L.W. van R., V.M, Y.M, T.J.M.W. performed writing, review and revision of the paper; All authors read and approved the final paper.

Funds

This work was supported by a grant from Stichting de Weijerhorst (Bewegen zonder Pijn), and grants from the Dutch Arthritis Foundation (grants 17-2-401 and LLP14). Mandy Peffers is funded through a Wellcome Trust Clinical Intermediate Fellowship (grant 107471/Z/15/Z) and supported by Versus Arthritis as part of the MRC Versus Arthritis Centre for Integrated research into Musculoskeletal Ageing (CIMA).

Declaration of competing interest

The authors declare no competing interests that are relevant to the submitted work.

Abbreviations

2′-O-me	2′-O-methylation
A–A	antibiotic-antimycotic
ANOVA	analysis of variance
ANS	anisomycin
AP1G1	adaptor related protein complex 1 subunit gamma 1
BCA	bicinchoninic acid
CHX	cycloheximide
CPM	counts per minute
DE	differentially expressed
DLR	dual-luciferase
DMEM/F-12	Dulbecco's modified eagle medium/nutrient mixture F-12
dTTP	deoxythymidine triphosphate
ELISA	enzyme-linked immunoassay
EMT	emetine
FA	fusidic acid
FBL	fibrillarin
FC	fold change

FCS	fetal calf serum
gDNA	genomic DNA
GFP	green fluorescent protein
sgRNA	single guide RNA
HAC	human articular chondrocyte
KCl	potassium chloride
KO	knockout
M	male
$MgCl_2$	magnesium chloride
NaCl	sodium chloride
NPM1	nucleophosmin
nm	nanometer
OA	osteoarthritis
OA-SF	osteoarthritic synovial fluid
PBS	phosphate buffered saline
RLU	relative light unit
RIN	RNA integrity number
RIPA	radioimmunoprecipitation assay
rRNA	ribosomal RNA
RT-qPCR	quantitative reverse transcription polymerase chain reaction
snoRNA	small nucleolar RNA

Supplementary data

Supplementary data to this article can be found online at https://doi.org/10.1016/j.joca.2022.12.010.

References

1. Trachana V, Mourmoura E, Papathanasiou I, Tsezou A. Understanding the role of chondrocytes in osteoarthritis: utilizing proteomics. Expert Rev Proteom 2019 Mar;16(3):201–13.
2. Gay DM, Lund AH, Jansson MD. Translational control through ribosome heterogeneity and functional specialization. Trends Biochem Sci 2022 Jan;47(1):66–81.
3. Khatter H, Myasnikov AG, Natchiar SK, Klaholz BP. Structure of the human 80S ribosome. Nature 2015 Apr 30;520(7549):640–5.
4. Steitz TA, Moore PB. RNA, the first macromolecular catalyst: the ribosome is a ribozyme. Trends Biochem Sci 2003 Aug;28(8):411–8.
5. Sloan KE, Warda AS, Sharma S, Entian KD, Lafontaine DLJ, Bohnsack MT. Tuning the ribosome: the influence of rRNA modification on eukaryotic ribosome biogenesis and function. RNA Biol 2017 Sep 2;14(9):1138–52.
6. Taoka M, Nobe Y, Yamaki Y, Sato K, Ishikawa H, Izumikawa K, *et al*. Landscape of the complete RNA chemical modifications in the human 80S ribosome. Nucleic Acids Res 2018 Oct 12;46(18):9289–98.
7. Motorin Y, Quinternet M, Rhalloussi W, Marchand V. Constitutive and variable 2'-O-methylation (Nm) in human ribosomal RNA. RNA Biol 2021 Sep 10:1–10.
8. Kiss-Laszlo Z, Henry Y, Bachellerie JP, Caizergues-Ferrer M, Kiss T. Site-specific ribose methylation of preribosomal RNA: a novel function for small nucleolar RNAs. Cell 1996 Jun 28;85(7):1077–88.
9. Jaafar M, Paraqindes H, Gabut M, Diaz JJ, Marcel V, Durand S. 2'O-Ribose methylation of ribosomal RNAs: natural diversity in living organisms, biological processes, and diseases. Cells 2021 Jul 31;10(8).
10. Jansson MD, Hafner SJ, Altinel K, Tehler D, Krogh N, Jakobsen E, *et al*. Regulation of translation by site-specific ribosomal RNA methylation. Nat Struct Mol Biol 2021 Nov;28(11):889–99.
11. van den Akker GGH, Zacchini F, Housmans BAC, van der Vloet L, Caron MMJ, Montanaro L, *et al*. Current practice in bicistronic IRES reporter use: a systematic review. Int J Mol Sci 2021 May 14;(10):22.
12. Ayadi L, Motorin Y, Marchand V. Quantification of 2'-O-Me residues in RNA using next-generation sequencing (Illumina RiboMethSeq protocol). Methods Mol Biol 2018;1649:29–48.
13. Marchand V, Blanloeil-Oillo F, Helm M, Motorin Y. Illumina-based RiboMethSeq approach for mapping of 2'-O-Me residues in RNA. Nucleic Acids Res 2016 Sep 19;44(16):e135.
14. Berman HM, Westbrook J, Feng Z, Gilliland G, Bhat TN, Weissig H, *et al*. The protein data bank. Nucleic Acids Res 2000 Jan 1;28(1):235–42.
15. Natchiar SK, Myasnikov AG, Kratzat H, Hazemann I, Klaholz BP. Visualization of chemical modifications in the human 80S ribosome structure. Nature 2017 Nov 23;551(7681):472–7.
16. Sanjana NE, Shalem O, Zhang F. Improved vectors and genome-wide libraries for CRISPR screening. Nat Methods 2014 Aug;11(8):783–4.
17. Pauli C, Liu Y, Rohde C, Cui C, Fijalkowska D, Gerloff D, *et al*. Site-specific methylation of 18S ribosomal RNA by SNORD42A is required for acute myeloid leukemia cell proliferation. Blood 2020 Jun 4;135(23):2059–70.
18. Di Ceglie I, van den Akker GG, Ascone G, Ten Harkel B, Hacker H, van de Loo FA, *et al*. Genetic modification of ER-Hoxb8 osteoclast precursors using CRISPR/Cas9 as a novel way to allow studies on osteoclast biology. J Leukoc Biol 2017 Apr;101(4):957–66.
19. Shalem O, Sanjana NE, Hartenian E, Shi X, Scott DA, Mikkelson T, *et al*. Genome-scale CRISPR-Cas9 knockout screening in human cells. Science 2014 Jan 3;343(6166):84–7.
20. Ripmeester EGJ, Caron MMJ, van den Akker GGH, Surtel DAM, Cremers A, Balaskas P, *et al*. Impaired chondrocyte U3 snoRNA expression in osteoarthritis impacts the chondrocyte protein translation apparatus. Sci Rep 2020 Aug 10;10(1), 13426.
21. Anderson JR, Smagul A, Simpson D, Clegg PD, Rubio-Martinez LM, Peffers MJ. The synovial fluid proteome differentiates between septic and nonseptic articular pathologies. J Proteom 2019 Jun 30;202, 103370.
22. Peffers MJ, Thorpe CT, Collins JA, Eong R, Wei TK, Screen HR, *et al*. Proteomic analysis reveals age-related changes in tendon matrix composition, with age- and injury-specific matrix fragmentation. J Biol Chem 2014 Sep 12;289(37):25867–78.
23. Peffers M, Liu X, Clegg P. Transcriptomic signatures in cartilage ageing. Arthritis Res Ther 2013 Aug 23;15(4):R98.
24. Panda AC, Martindale JL, Gorospe M. Polysome fractionation to analyze mRNA distribution profiles. Bio Protoc 2017 Feb 5;7(3).
25. Housmans BAC, Neefjes M, Surtel DAM, Vitik M, Cremers A, van Rhijn LW, *et al*. Synovial fluid from end-stage osteoarthritis induces proliferation and fibrosis of articular chondrocytes via MAPK and RhoGTPase signaling. Osteoarthr Cartil 2022 Feb 15;30(6):862–74.
26. Nazar RN, Lo AC, Wildeman AG, Sitz TO. Effect of 2'-O-methylation on the structure of mammalian 5.8S rRNAs and the 5.8S-28S rRNA junction. Nucleic Acids Res 1983 Sep 10;11(17):5989–6001.
27. Marcel V, Kielbassa J, Marchand V, Natchiar KS, Paraqindes H, Nguyen Van Long F, *et al*. Ribosomal RNA 2'O-methylation as a novel layer of inter-tumour heterogeneity in breast cancer. NAR Cancer 2020 Dec;2(4):zcaa036.
28. Munholland JM, Nazar RN. Methylation of ribosomal RNA as a possible factor in cell differentiation. Cancer Res 1987 Jan 1;47(1):169–72.

29. Nazar RN, Sitz TO, Busch H. Tissue specific differences in the 2'-O-methylation of eukaryotic 5.8S ribosomal RNA. FEBS Lett 1975 Nov 1;59(1):83–7.
30. Huttenhofer A, Kiefmann M, Meier-Ewert S, O'Brien J, Lehrach H, Bachellerie JP, *et al*. RNomics: an experimental approach that identifies 201 candidates for novel, small, non-messenger RNAs in mouse. EMBO J 2001 Jun 1;20(11):2943–53.
31. Dmitriev SE, Vladimirov DO, Lashkevich KA. A quick guide to small-molecule inhibitors of eukaryotic protein synthesis. Biochemistry 2020 Nov;85(11):1389–421.
32. Lestrade L, Weber MJ. snoRNA-LBME-db, a comprehensive database of human H/ACA and C/D box snoRNAs. Nucleic Acids Res 2006 Jan 1;34(Database issue):D158–62.
33. Helser TL, Baan RA, Dahlberg AE. Characterization of a 40S ribosomal subunit complex in polyribosomes of Saccharomyces cerevisiae treated with cycloheximide. Mol Cell Biol 1981 Jan;1(1):51–7.
34. Wong W, Bai XC, Brown A, Fernandez IS, Hanssen E, Condron M, *et al*. Cryo-EM structure of the Plasmodium falciparum 80S ribosome bound to the anti-protozoan drug emetine. Elife 2014 Jun 9:3.
35. Mazumder R. Sites of action of fusidic acid in eukaryotes. Inhibition by fusidic acid of a ribosome-independent GTPase from Artemia salina embryos. Eur J Biochem 1975 Oct 15;58(2):549–54.
36. Tafforeau L, Zorbas C, Langhendries JL, Mullineux ST, Stamatopoulou V, Mullier R, *et al*. The complexity of human ribosome biogenesis revealed by systematic nucleolar screening of Pre-rRNA processing factors. Mol Cell 2013 Aug 22;51(4):539–51.
37. Weingarten-Gabbay S, Elias-Kirma S, Nir R, Gritsenko AA, Stern-Ginossar N, Yakhini Z, *et al*. Comparative genetics. Systematic discovery of cap-independent translation sequences in human and viral genomes. Science 2016 Jan 15;(6270):351.
38. Godet AC, David F, Hantelys F, Tatin F, Lacazette E, Garmy-Susini B, *et al*. IRES trans-acting factors, key actors of the stress response. Int J Mol Sci 2019 Feb 20;20(4).
39. van den Akker GGH, Caron MMJ, Peffers MJ, Welting TJM. Ribosome dysfunction in osteoarthritis. Curr Opin Rheumatol 2022 Jan 1;34(1):61–7.
40. Jaafar ZA, Oguro A, Nakamura Y, Kieft JS. Translation initiation by the hepatitis C virus IRES requires eIF1A and ribosomal complex remodeling. Elife 2016 Dec 23:5.
41. Penzo M, Montanaro L. Turning uridines around: role of rRNA pseudouridylation in ribosome biogenesis and ribosomal function. Biomolecules 2018 Jun 5;8(2).
42. Yusupov MM, Yusupova GZ, Baucom A, Lieberman K, Earnest TN, Cate JH, *et al*. Crystal structure of the ribosome at 5.5 A resolution. Science 2001 May 4;292(5518):883–96.
43. Abou Elela S, Good L, Melekhovets YF, Nazar RN. Inhibition of protein synthesis by an efficiently expressed mutation in the yeast 5.8S ribosomal RNA. Nucleic Acids Res 1994 Feb 25;22(4):686–93.
44. Abou Elela S, Nazar RN. Role of the 5.8S rRNA in ribosome translocation. Nucleic Acids Res 1997 May 1;25(9):1788–94.
45. Walker K, Elela SA, Nazar RN. Inhibition of protein synthesis by anti-5.8 S rRNA oligodeoxyribonucleotides. J Biol Chem 1990 Feb 15;265(5):2428–30.
46. Talkish J, Campbell IW, Sahasranaman A, Jakovljevic J, Woolford Jr JL. Ribosome assembly factors Pwp1 and Nop12 are important for folding of 5.8S rRNA during ribosome biogenesis in Saccharomyces cerevisiae. Mol Cell Biol 2014 May;34(10):1863–77.
47. Ji Q, Zheng Y, Zhang G, Hu Y, Fan X, Hou Y, *et al*. Single-cell RNA-seq analysis reveals the progression of human osteoarthritis. Ann Rheum Dis 2019 Jan;78(1):100–10.
48. Rim YA, Ju JH. The role of fibrosis in osteoarthritis progression. Life 2020 Dec 23;11(1).
49. Caron MMJ, Ripmeester EGJ, van den Akker G, Wijnands N, Steijns J, Surtel DAM, *et al*. Discovery of bone morphogenetic protein 7-derived peptide sequences that attenuate the human osteoarthritic chondrocyte phenotype. Mol Ther Methods Clin Dev 2021 Jun 11;21:247–61.
50. Housmans BAC, van den Akker GGH, Neefjes M, Timur UT, Cremers A, Peffers MJ, *et al*. Direct comparison of non-osteoarthritic and osteoarthritic synovial fluid-induced intracellular chondrocyte signaling and phenotype changes. Osteoarthr Cartil 2023 Jan;31(1):60–71.
51. Bailey AD, Talkish J, Ding H, Igel H, Duran A, Mantripragada S, *et al*. Concerted modification of nucleotides at functional centers of the ribosome revealed by single-molecule RNA modification profiling. Elife 2022 Apr 6:11.
52. Deryusheva S, Talross GJS, Gall JG. SnoRNA guide activities: real and ambiguous. RNA 2021 Nov;27(11):1363–73.
53. Nwagwu M, Nana M. Ribonucleic acid synthesis in embryonic chick muscle, rates of synthesis and half-lives of transfer and ribosomal RNA species. J Embryol Exp Morphol 1980 Apr;56:253–67.
54. Yang E, van Nimwegen E, Zavolan M, Rajewsky N, Schroeder M, Magnasco M, *et al*. Decay rates of human mRNAs: correlation with functional characteristics and sequence attributes. Genome Res 2003 Aug;13(8):1863–72.